catalysts

MDPI

Article

Synthesis of NaOH-Modified $TiOF_2$ and Its Enhanced Visible Light Photocatalytic Performance on RhB

Chentao Hou *, Wenli Liu and Jiaming Zhu

College of Geology and Environment, Xi'an University of Science and Technology, Xi'an 710054, China; 13572955186@163.com (W.L.); XRD610@126.com (J.Z.)

* Correspondence: houct@xust.edu.cn; Tel.: +86-029-8558-3188

Received: 16 July 2017; Accepted: 16 August 2017; Published: 22 August 2017

Abstract: NaOH-modified $TiOF_2$ was successfully prepared using a modified low-temperature hydrothermal method. Scanning electron microscopy shows that NaOH-modified $TiOF_2$ displayed a complex network shape with network units of about 100 nm. The structures of NaOH-modified $TiOF_2$ have not been reported elsewhere. The network shape permits the NaOH-modified $TiOF_2$ a S_{BET} of 36 $m^2 \cdot g^{-1}$ and a pore diameter around 49 nm. X-ray diffraction characterization shows that $TiOF_2$ and NaOH-modified $TiOF_2$ are crystallized with a pure changed cubic phase which accords with the SEM results. Fourier transform infrared spectroscopy characterization shows that NaOH-modified $TiOF_2$ has more O–H groups to supply more lone electron pairs to transfer from O of O–H to Ti and O of $TiOF_2$. UV–vis diffuse reflectance spectroscopy (DRS) shows that the NaOH-modified $TiOF_2$ sample has an adsorption plateau rising from 400 to 600 nm in comparison with $TiOF_2$, and its band gap is 2.62 eV, lower than that of $TiOF_2$. Due to the lower band gap, more O–H groups adsorption, network morphologies with larger surface area, and sensitization progress, the NaOH-modified $TiOF_2$ exhibited much higher photocatalytic activity for Rhodamine B (RhB) degradation. In addition, considering the sensitization progress, O–H groups on $TiOF_2$ not only accelerated the degradation rate of RhB, but also changed its degradation path. As a result, the NaOH-modified $TiOF_2$ exhibited much higher photocatalytic activity for RhB degradation than the $TiOF_2$ in references under visible light. This finding provides a new idea to enhance the photocatalytic performance by NaOH modification of the surface of $TiOF_2$.

Keywords: $TiOF_2$; NaOH-modified $TiOF_2$; network shape; photocatalysis; RhB

1. Introduction

Nowadays, environmental pollution is affecting human survival and development. Photocatalysis is considered an efficient, stable, and environmentally friendly method for controlling environmental pollution [1]. In the past, TiO_2 has been widely used as a photocatalyst in the photo-degradation of organic pollutants. However, it has a wide energy band gap (3.1–3.2 eV) which only permit its UV light response and can easily cause electron–hole recombination [1–4]. Thus, studies on changing morphology [1–3], modification [1,4,5], and other methods were conducted to decrease its band gap or inhibit its electron–hole recombination. The discovery of non-titanium semiconductor photocatalysts with a narrow intrinsic energy band gap, efficiently driven by visible light, may also attract much attention [5–13].

Recently, Li's research group found that $TiOF_2$ cubes—considered a promising anode material for lithium ion batteries (LIBs) [14–19]—showed visible-light driven property and exhibited excellent performance in photodegradation of Rhodamine B (RhB) and 4-chlorophenol (4-CP) [7]. $TiOF_2$ is also proven to be more active and durable at room temperature due to the covalent bonds of F species with Ti [8,9]. Only a few studies focused on the photocatalytic activity of $TiOF_2$ have been reported [7–9].

As usual, $TiOF_2$ nanoparticles were synthesized via hydrothermal [10,14–18] and solvothermal [7,11,12] methods from titanium (IV) isopropoxide (TIP), and have a cubic shape [7–18]. The size of $TiOF_2$ nanocubes could be affected by alcoholysis time, alcohol kind, solvothermal temperature, different H_2O production rate and amount [7,17]. While the photocatalytic activity of $TiOF_2$ is still unsatisfactory, it is necessary to explore novel approaches to improve its photocatalytic performance.

Alkali modification is proven to be an effective method to enhance the catalytic performance for α-pinene isomerization, formaldehyde oxidation, and benzene hydroxylation [20–23]. Thus, it stimulated us to modify the $TiOF_2$ catalyst obtained from our earlier studies. In this study, we firstly reported a network-shaped NaOH-modified $TiOF_2$ treated by a hydrothermal process under low temperature. The FTIR measurement showed that more associated O–H exists on the surface of $TiOF_2$, which can remarkably enhance the catalytic activity of $TiOF_2$ toward RhB oxidation under visible light. The NaOH-modified $TiOF_2$ had better photocatalytic performance than $TiOF_2$ in Li's research [7].

2. Results and Discussion

2.1. Phase Structures and Morphology

The phase and crystallinity of the as-prepared $TiOF_2$ and NaOH-modified $TiOF_2$ samples were tested by XRD analysis. It can be seen from Figure 1, the patterns of as-prepared $TiOF_2$ and NaOH-modified $TiOF_2$ samples all have sharp peaks at 2θ = 23.6°, 48.1°, and 54.2°, corresponding to the (100), (200), and (210) planes of the cubic $TiOF_2$ phase (JCPDS no. 08-0060) [7,13] and no peak of any anatase TiO_2 (JCPDS no. 21-1272) [24,25] crystal appears, indicating that the as-prepared samples have high crystallinity and pure phase of cubic $TiOF_2$. It also indicates that the height of the (100) crystal planes of the $TiOF_2$ and NaOH-modified $TiOF_2$ are higher, and the (200) and (210) crystal planes are lower than that of the standard cubic $TiOF_2$, indicating a new shape of the as-prepared $TiOF_2$ and NaOH-modified $TiOF_2$. The Scherrer formula was used to calculate the normal distance of certain crystal surfaces of $TiOF_2$ and NaOH-modified $TiOF_2$

$$\tau = \kappa\lambda/(\beta\cos\theta) \tag{1}$$

where τ, κ, λ, β, and θ are the mean normal distance of certain crystal surfaces, the shape constant with a value of 0.89 when β is the half width of the diffraction peak (FWHM), the diffracted ray wavelength (0.15418 nm for Cu-Ka), and the diffraction angle in radians, respectively [26].

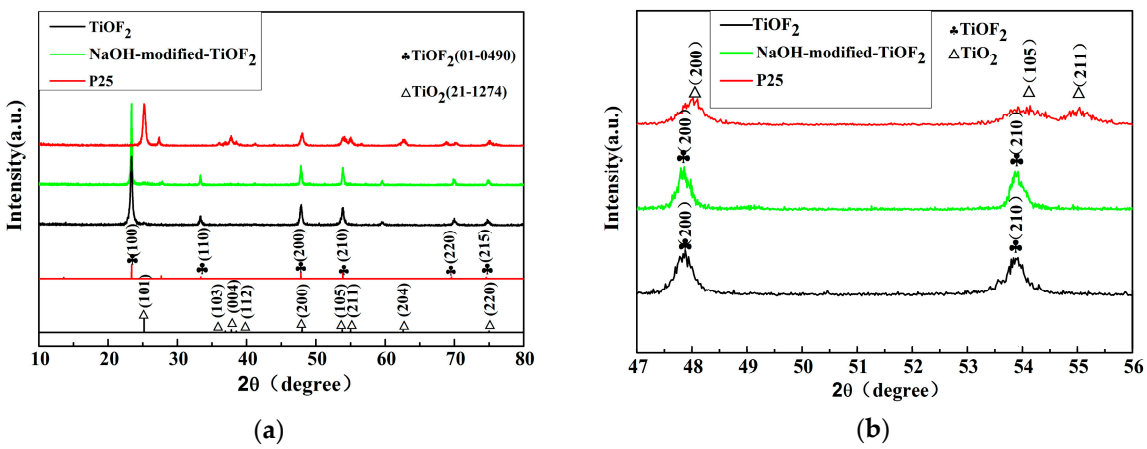

Figure 1. XRD pattern with 2θ from 10° to 80° (**a**) and partial enlarged detail of 2θ from 47° to 56° (**b**) of as-prepared $TiOF_2$, NaOH-modified $TiOF_2$, commercial P25 and a standard card of $TiOF_2$ and TiO_2.

The normal distances of $TiOF_2$ are 7.26, 17.81, 11.67, 10.77, 17.38, and 16.98 nm along the (100), (110), (200), (210), (220), and (215) planes [7,13], respectively, while the distanced of crystal

NaOH-modified $TiOF_2$ change to 15.99, 42.18, 26.26, 30.78, 40.80, and 48.39 nm along the corresponding planes, respectively. It can be seen that the normal distance of the crystalline phase of NaOH-modified $TiOF_2$ shrunk 8.88% and 3.72% along (100) and (110) planes. However, an increase was observed along (200), (210), and (215) planes. This can be explained in that NaOH-modifying induces more O–H adsorbed onto (100) and (110) planes of $TiOF_2$ and, thus, induces the planes' exposure.

Morphologies and microstructure of original $TiOF_2$ and NaOH-modified $TiOF_2$ were checked by SEM characterization. In Figure 2a,b, $TiOF_2$ crystals displayed a mixture of the cubic image which is accords with the cubic image in [7–18]. Each individual particle crystal is about 50–300 nm and tends to aggregate, forming larger particles while—in Figure 2c,d—the NaOH-modified $TiOF_2$ displayed a more complex network shape with network units in about 100 nm. The NaOH-modified $TiOF_2$ shows phases assembling along certain directions. This accords with the XRD results. The network shape permits much more surface area for photocatalysis. These structures of NaOH-modified $TiOF_2$ have not been reported elsewhere. The Barrett-Joyner-Halenda (BJH) method was used to analyze the pore size distribution and pore volume and the surface area (S_{BET}) was calculated using the BET method. The Figure 3a demonstrated that the NaOH-modified $TiOF_2$ showed a typical IV type N_2 adsorption–desorption isotherm and mesoporous structure with an average pore diameter of about 49 nm. Thus, its S_{BET} can reach as high as 36 $m^2 \cdot g^{-1}$, while the average pore diameter and S_{BET} of $TiOF_2$ are only 3 nm and 2.7 $m^2 \cdot g^{-1}$, which is much lower than that of NaOH-modified $TiOF_2$. The larger surface area permits more O–H and pollutant adsorption and the formation of additional mesopores affects the improvement of mass transfer, enhancing photocatalytic performance accordingly [21,22].

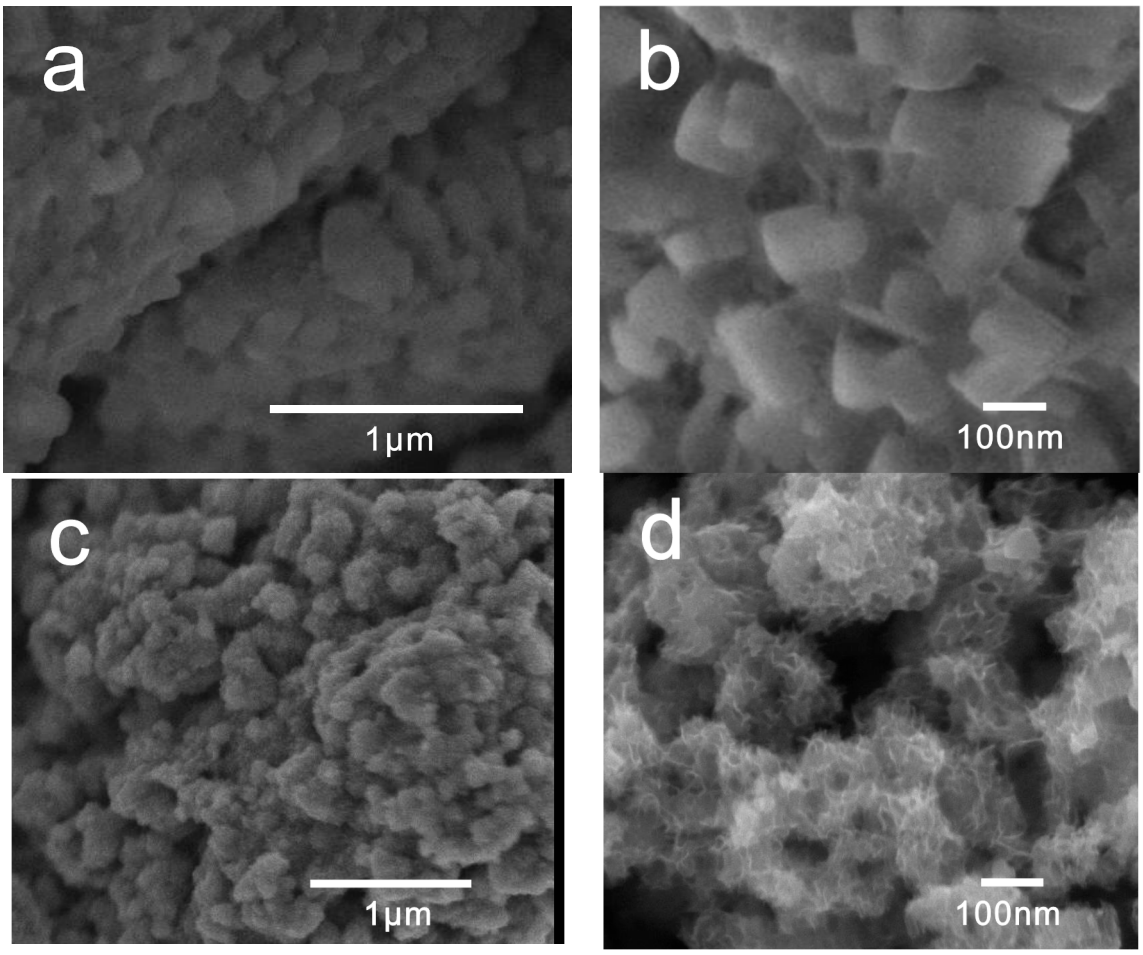

Figure 2. SEM of as-synthesized samples: (**a**,**b**) $TiOF_2$; and (**c**,**d**) NaOH-modified $TiOF_2$.

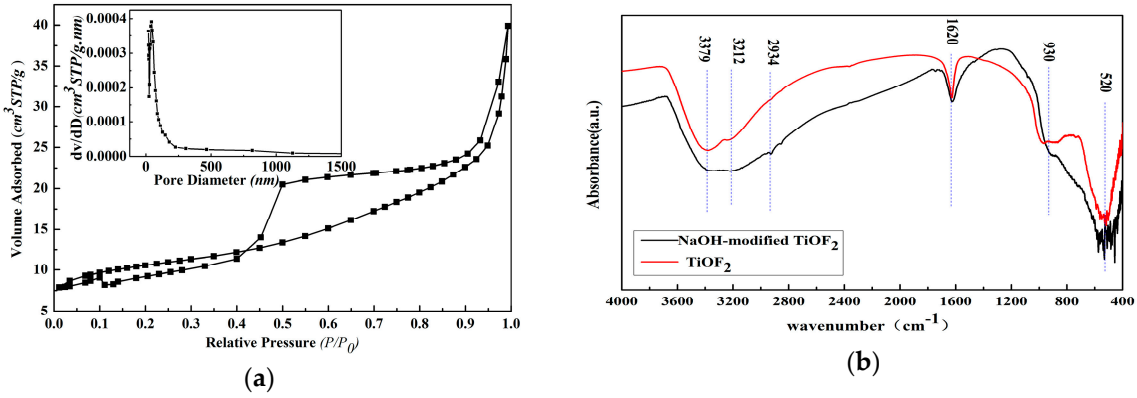

Figure 3. N_2 adsorption-desorption isotherm of the NaOH-modified $TiOF_2$ (**a**) and the FTIR spectra for $TiOF_2$ and NaOH-modified TiOF (**b**).

2.2. FTIR Analysis

Figure 3b shows the FTIR spectra of $TiOF_2$ and NaOH-modified $TiOF_2$. The strong band around 700–500 cm^{-1} could contribute to the Ti–O–Ti stretching vibration [22–24]. The peak around 3379 cm^{-1} and the broad band centered around 3212 cm^{-1} were due to the free and bonding O–H stretching vibration of Ti−OH, respectively [27,28]. The peak at 1620 cm^{-1} was due to the O–H bending vibration of Ti−OH [16,22,29–33]. The broad band centered around 3212 cm^{-1} in NaOH-modified $TiOF_2$ becomes broader than that in $TiOF_2$, meaning that more O–H bonds or associated O–H appeared in NaOH-modified $TiOF_2$. According to previous work, the free O–H stretching vibration used to appear at about 3600 cm^{-1} without bonding O–H [27,28]. It can be seen that the O–H frequency for $TiOF_2$ and NaOH-modified $TiOF_2$ is 221 cm^{-1} and 388 cm^{-1} lower than 3600 cm^{-1}, indicating a strong hydrogen bond impact [27,28]. The O–H on the TiO_2 surface can enhance the transference of photo-generated electrons and then enhance photocatalytic performance [29]. The peaks around 930 cm^{-1} were due to the Ti–F vibrations in the $TiOF_2$ [16]. The peak intensity decreased from $TiOF_2$ to NaOH-modified $TiOF_2$, indicating F was exchanged by O–H after NaOH modification. All of these show that the NaOH-modified $TiOF_2$ samples contain more O–H groups than $TiOF_2$. It can be explained that $TiOF_2$ was modified in NaOH solution, thus, more O–H would be chemisorbed onto $TiOF_2$, and further exchanged with F. Then, more lone pair electrons in the O–H groups transferring from the O of O–H to Ti and the O of $TiOF_2$, the performance of $TiOF_2$ can be enhanced accordingly [21]. In addition, because RhB is a cationic dye, NaOH brings more O–H onto the surface of $TiOF_2$ to hold more RhB and accelerate its degradation rate [34,35].

2.3. UV–Vis Analysis

Figure 4 shows that the UV–vis absorption spectroscopy and band gap of as-prepared $TiOF_2$ and NaOH-modified $TiOF_2$ samples. The NaOH-modified $TiOF_2$ has a raised adsorption plateau from 400 to 600 nm, which indicates stronger visible light absorption than that of $TiOF_2$ (Figure 4a). Band gap estimation can be seen in Figure 4b showing that the band gap of NaOH-modified $TiOF_2$ is 2.62 eV, which is lower than that of $TiOF_2$ (2.80 eV) and lower than anatase TiO_2 (3.2 eV) [1–4], NiO (4.0 eV) [6], and other oxides, indicating easier excitation by visible light. This can be explained in that NaOH treatment causes certain facet exposure and network morphologies of $TiOF_2$, changing its light absorption properties. Thus, the NaOH treatment lowered the band gap of $TiOF_2$, enhanced its visible light absorption, and further enhanced its visible light photocatalytic properties.

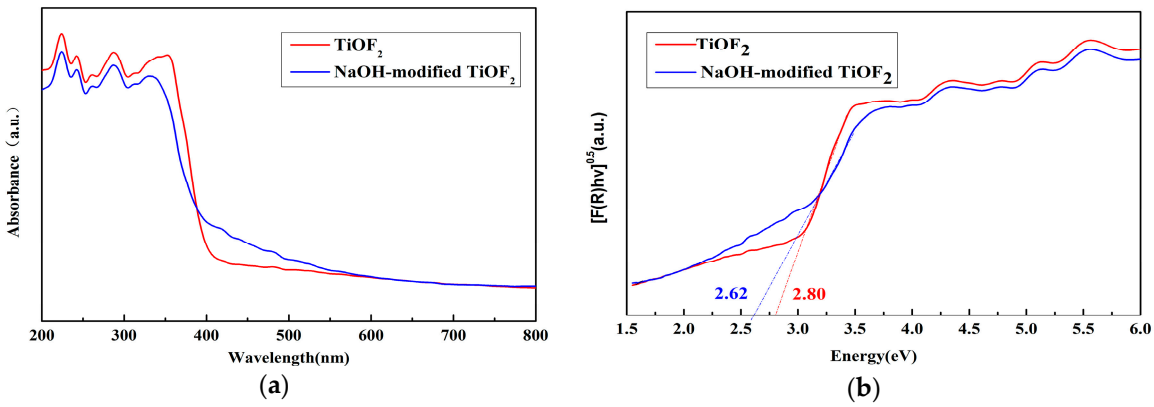

Figure 4. UV–vis DRS spectra (**a**) and band gap (**b**) of $TiOF_2$ and NaOH-modified $TiOF_2$.

2.4. Catalytic Activity

Figure 5 shows the visible light photcatalytic properties of $TiOF_2$, NaOH-modified $TiOF_2$, $TiOF_2$ in reference ($TiOF_2$-Ref) [7,13], $TiOF_2$-crushed in reference ($TiOF_2$-crushed-Ref) [7], and P25. It can be seen in Figure 5a that, in the adsorption test in dark and in light on the process without the catalyst for RhB, the decrease of RhB is very small. It can be concluded that the adsorption and sensitization mechanisms can be negligible in the degradation process. Thus, the degradation of RhB was a photocatalytic process. The concentration of RhB decreased under the same conditions, which means that all samples are visible-light active. It also shows that NaOH-modified $TiOF_2$ can cause almost complete decomposition of RhB in 3 h, having better photocatalytic performance than all of the $TiOF_2$ in reference [7,13]. While P25 and $TiOF_2$ performed poorly compared to NaOH-modified $TiOF_2$ and $TiOF_2$-Ref. The reaction rate of all of the samples are shown in Figure 5b. It can be seen that the data was fitted with the first-order reaction equation as

$$\ln(C_0/C) = kt \tag{2}$$

where t is the reaction time, C_0 is concentration of RhB at time 0, C is the concentration of RhB at time t, and k is the reaction rate constant.

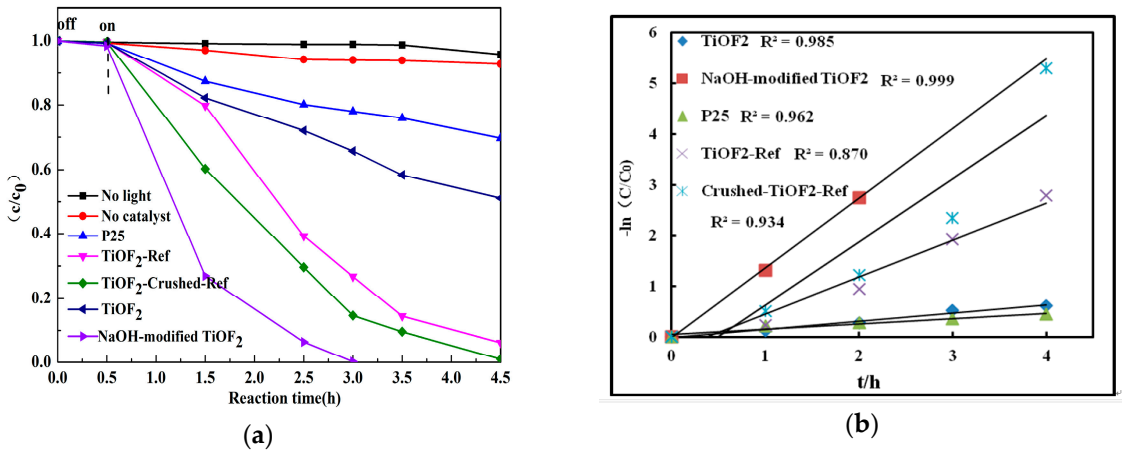

Figure 5. Catalytic activity of RhB under visible light: (**a**) concentration dependent on time and (**b**) kinetic fit for the degradation of RhB.

It can be seen that P25 and $TiOF_2$ had rate constants of only 0.10 and 0.16 h^{-1}, indicating poor photocatalytic performance. The result is consistent with previous work [8,20]. The calculated rate

constants are 1.37, 0.73, and 1.24 h^{-1} for NaOH-modified $TiOF_2$, $TiOF_2$-Ref, and $TiOF_2$-crushed-Ref, respectively. The NaOH-modified $TiOF_2$ sample shows the best performance among all the photocatalysts, whose degradation rates are much higher than that of P25 and $TiOF_2$ in our samples and 10.4% higher than that of $TiOF_2$-crushed-Ref The excellent performance could be mainly attributed to its larger S_{BET} (32 $m^2 \cdot g^{-1}$ for $TiOF_2$-crushed-Ref) and more bonding O–H [7,21].

2.5. Effect of the Sensitization Mechanism

According to previous studies, dyes can be degraded on TiO_2 through a sensitized process under visible light [34,35]. In order to know whether there is a similar path on $TiOF_2$ and NaOH-modified $TiOF_2$, UV–vis absorption spectral changes of RhB with visible light irradiation time in the suspension of $TiOF_2$ and NaOH-modified $TiOF_2$ were tested. The results are shown in Figure 6. It can be seen in Figure 6 that the spectral change of RhB with the irradiation time on NaOH-modified $TiOF_2$ is quite different from that on $TiOF_2$. There is a blue-shift from 558 to 498 nm in the absorption maximum with irradiation time for NaOH-modified $TiOF_2$, while none in that of $TiOF_2$. This is attributed to the N-deethylation products of RhB, which confirms the possibility of the sensitization mechanism [34,35]. Thus, NaOH treatment can induce the sensitization process and change the degradation path of $TiOF_2$.

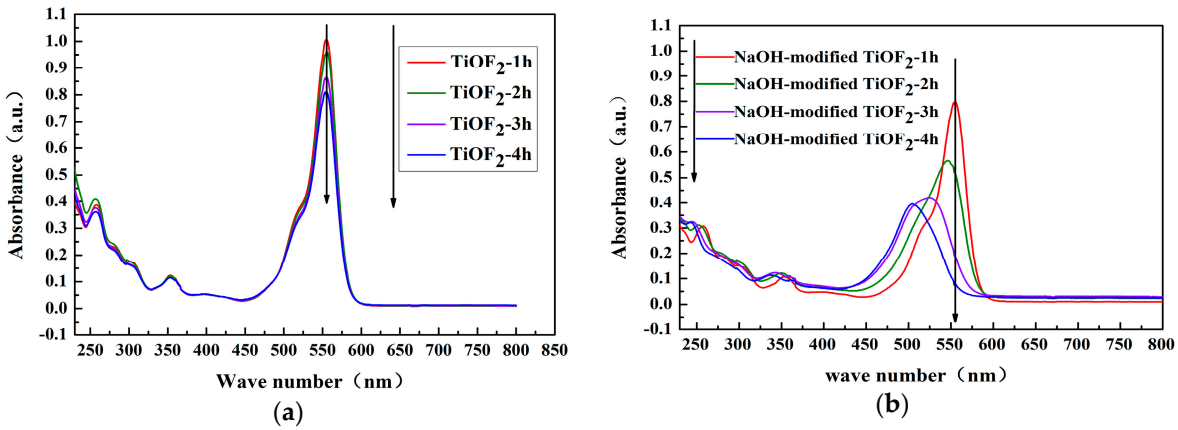

Figure 6. UV–vis absorption spectra of RhB in (**a**) $TiOF_2$ and (**b**) NaOH-modified $TiOF_2$ suspension under visible light.

3. Materials and Methods

Tetrabutyl titanate (TBOT, A.R. grade) was purchased from Fu Chen Chemical Reagent Factory, Tianjin, China. Absolute ethyl alcohol (C_2H_5OH, A.R. grade) and sodium hydroxide (NaOH, A.R. grade) was purchased from Fuyu Fine Chemical Co., Ltd., Tianjin, China. Hydrofluoric acid (HF, A.R. grade) was purchased from Xilong Chemical Industry Co., Ltd., Chengdu, China. All reagents are used without further purification. Ultrapure water was used as the experimental water.

NaOH-modified $TiOF_2$ was synthesized via a modified low-temperature hydrothermal method. In a typical synthesis, 30.4 mL absolute ethyl alcohol was added into 35.2 mL TBOT, which was named solution A. Absolute ethyl alcohol (30.4 mL) and 20.2 mL HF were added into 180 mL ultrapure water, which was named solution B. Solution A was dropped into solution B under medium-speed magnetic stirring at 20 °C for 1.5 h to obtain a faint yellow sol. The sol was aged at room temperature for 2 days to change to a gel. The gel was then transferred into a 50-mL Teflon-lined stainless steel autoclave. When sealed, the autoclave was placed at 100 °C for 2 h in a drying box, then was naturally cooled to room temperature. Ultra-pure water and absolute ethanol were used to wash the obtained white precipitates several times to reach a pH of 7, and then the precipitates were dried at 100 °C. The as-prepared sample was $TiOF_2$. One gram of the $TiOF_2$ precursor was dispersed in 100 mL 5 $mol \cdot L^{-1}$ NaOH solution under magnetic stirring with a speed of 4000 $r \cdot min^{-1}$ for 1 h, then the suspension was also washed with ultra-pure water and absolute ethanol to reach a pH

of 7. The product was dried at 100 °C for 12 h. The sample was denoted as NaOH-modified $TiOF_2$. The crystal structure as analyzed by a XD-2 X-ray diffractometer (Beijing Purkinje, Beijing, China) with Cu Kαradiation with a scan rate of $4.0000° \cdot min^{-1}$. The morphology was examined by field emission scanning electron microscopy (FESEM, JEOL JSM6700, Tokyo, Japan). Fourier transform infrared (FTIR) spectra were recorded using a Bruker TENSOR27 (Karlsurhe, Germeny) using the KBr method. The optical properties were determined by UV–vis diffuse reflectance spectroscopy (UV–vis DRS: (Shimadzu 2600, Beijing, China). N_2 adsorption-desorption isotherms were measured at 77 K and the BET method was used to calculate the surface area (S_{BET}) by a JW-BK122F (Beijing, China).

The degradation of RhB was conducted at room temperature in a 150 mL double-layered quartz reactor containing 50 mg catalyst and 50 mL 5.0 $mg \cdot L^{-1}$ RhB solution. A 300 W Xe lamp (Jiguang-300, Shanghai, China) was located at a distance of 15 cm from the RhB solution to simulate solar light. A cutoff filter (JB-420, Shanghai, China) was chosen to filter off the light whose wavelength was less than 420 nm to simulate visible light. The solution was magnetically stirred for 30 min to ensure the adsorption–desorption equilibrium, then the xenon lamp was turned on to start the photocatalytic degradation. At 30 min time intervals, about 5.0 mL RhB solution was extracted and centrifuged at high-speed (11,000 $r \cdot min^{-1}$) to remove catalysts. Then the concentration of the remaining RhB solutions were analyzed with a Purkinje UV1901 UV–vis spectrophotometer at 554 nm. The photocatalyst was separated from the RhB solution and another run of the reaction was started to investigate the durability of the catalysts.

4. Conclusions

NaOH-modified $TiOF_2$ was successfully prepared via a modified low-temperature solvothermal method. It exhibited much better photocatalytic performance for RhB degradation. XRD characterization shows that $TiOF_2$ and NaOH-modified $TiOF_2$ are crystallized with a pure changed cubic phase which is accord with the SEM results. SEM shows that $TiOF_2$ crystals displayed a mixture of the cubic images, while the NaOH-modified $TiOF_2$ displayed a more complex network shape with network units in about 100 nm. These structures of NaOH-modified $TiOF_2$ have not been reported elsewhere. The network shape permits the NaOH-modified $TiOF_2$ a surface area of 36 $m^2 \cdot g^{-1}$ and a pore diameter about 49 nm, which will enhance the adsorption of O–H groups and pollutants. FTIR characterization shows that NaOH-modified $TiOF_2$ has more O–H groups to supply more lone electron pairs transferring from O of the O–H groups to Ti and O of $TiOF_2$, in accordance with the BET analysis. UV–vis absorption spectroscopy shows that the NaOH-modified $TiOF_2$ samples have an adsorption plateau rising from 400 to 600 nm in comparison with $TiOF_2$ and its band gap is 2.62 eV, lower than that of $TiOF_2$. Due to the lower band gap, more O–H groups adsorption, network morphologies with larger surface area, and sensitization process, the NaOH-modified $TiOF_2$ exhibited much higher photocatalytic activity for RhB degradation. In addition, considering the sensitization process, O–H on $TiOF_2$ not only accelerated the degradation rate of RhB, but also changed its degradation path. This finding provides a new idea to enhance the photocatalytic performence by NaOH modification of the surface of $TiOF_2$. Considering its synthesizing process, the NaOH-modified $TiOF_2$ needs much lower temperature and shorter time than $TiOF_2$-crushed-Ref, but has much better photocatalytic performance, which provides a more economic choice.

Acknowledgments: Financial support was provided by Shaanxi Key Industrial Projects (2014GY2-07) and the Shaanxi Province Education Department Science and Technology Research Plan (15JK1460).

Author Contributions: In this paper, Chentao Hou and Wenli Liu designed the experiments; Wenli Liu and Jiaming Zhu conducted the experiments; Chentao Hou and Wenli Liu analyzed the data; and Chentao Hou wrote the article.

Conflicts of Interest: There is no conflict of interest existing in the manuscript submission, and it is approved by all of the authors for publication. All the authors listed have approved the manuscript to be enclosed.

References

1. Chen, X.; Mao, S.S. Titanium dioxide nanomaterials: Synthesis, properties, modifications, and applications. *Chem. Rev.* **2007**, *107*, 2891–2959. [CrossRef] [PubMed]
2. Nunes, D.; Pimentel, A.; Santos, L.; Barquinha, P.; Fortunato, E.; Martins, R. Photocatalytic TiO_2 Nanorod Spheres and Arrays Compatible with Flexible Applications. *Catalysts* **2017**, *7*, 60. [CrossRef]
3. Zuo, S.; Jiang, Z.; Liu, W.; Yao, C.; Chen, Q.; Liu, X. Synthesis and Characterization of Urchin-like Mischcrystal TiO_2 and Its Photocatalysis. *Mater. Charact.* **2014**, *96*, 177–182. [CrossRef]
4. Xie, C.; Yang, S.; Shi, J.; Niu, C. Highly Crystallized C-Doped MesoporousAnatase TiO_2 with Visible Light Photocatalytic Activity. *Catalysts* **2016**, *6*, 117. [CrossRef]
5. Cherian, C.T.; Reddy, M.V.; Magdaleno, T.; Sow, C.-H.; Ramanujachary, K.V.; Rao, G.V.S.; Chowdari, B.V.R. (N,F)-Co-doped TiO_2: Synthesis, anatase-rutile conversion and Li-cycling properties. *CrystEngComm* **2012**, *14*, 978–986. [CrossRef]
6. Ramasami, A.K.; Reddy, M.V.; Balakrishna, G.R. Combustion synthesis and characterization of NiO nanoparticles. *Mater. Sci. Semicond. Process.* **2015**, *40*, 194–202. [CrossRef]
7. Wang, J.; Cao, F.; Bian, Z.; Leung, M.K.H.; Li, H. Ultrafine single-crystal $TiOF_2$ nanocubes with mesoporous structure, high activity and durability in visible light driven photocatalysis. *Nanoscale* **2014**, *6*, 897–902. [CrossRef] [PubMed]
8. Wang, Z.; Ana, C.; Zhang, J. Synthesis of heterostructured Pd@TiO_2/$TiOF_2$ nanohybrids with enhanced photocatalytic performance. *Mater. Res. Bull.* **2016**, *80*, 337–343.
9. Dongn, P.; Cui, E.; Hou, G.; Guan, R.; Zhang, Q. Synthesis and photocatalytic activity of Ag_3PO_4/$TiOF_2$ composites with enhanced stability. *Mater. Lett.* **2015**, *143*, 20–23. [CrossRef]
10. Lv, K.; Yu, J.; Cui, L.; Chen, S.; Li, M. Preparation of thermally stable anatase TiO_2 photocatalyst from $TiOF_2$ precursor and its photocatalytic activity. *J. Alloys Compd.* **2011**, *509*, 4557–4562. [CrossRef]
11. Wang, Z.; Huang, B.; Dai, Y.; Zhang, X.; Qin, X.; Li, Z.; Zheng, Z.; Cheng, H.; Guo, L. Topotactic transformation of single-crystalline $TiOF_2$ nanocubes to ordered arranged 3D hierarchical TiO_2 nanoboxes. *CrystEngComm* **2012**, *14*, 4578–4581. [CrossRef]
12. Huang, Z.; Wang, Z.; Lv, K.; Zheng, Y.; Deng, K. Transformation of $TiOF_2$ cube to a hollow nanobox assembly from anatase TiO_2 nanosheets with exposed {001} facets via solvothermal strategy. *ACS Appl. Mater. Interfaces* **2013**, *5*, 8663–8669. [CrossRef] [PubMed]
13. Wen, C.Z.; Hu, Q.H.; Guo, Y.N.; Gong, X.Q.; Qiao, S.Z.; Yang, H.G. From titanium oxydifluoride ($TiOF_2$) to titania (TiO_2): Phase transition and non-metal doping with enhanced photocatalytic hydrogen (H_2) evolution properties. *Chem. Commun.* **2011**, *47*, 6138–6140. [CrossRef] [PubMed]
14. Jung, M.; Kim, Y.; Lee, Y. Enhancement of the electrochemical capacitance of $TiOF_2$ obtained via control of the crystal structure. *J. Ind. Eng. Chem.* **2017**, *47*, 187–193. [CrossRef]
15. Louvain, N.; Karkar, Z.; El-Ghozzi, M.; Bonnet, P.; Gúerin, K.; Willmann, P. Fluorinationof anatase TiO_2 towards titanium oxyfluoride $TiOF_2$: A novel synthesis approach and proof of the Li-insertion mechanism. *J. Mater. Chem. A* **2014**, *2*, 15308–15315. [CrossRef]
16. Li, W.; Body, M.; Legein, C.; Dambournet, D. Identify OH groups in $TiOF_2$ and their impact on the lithium intercalation properties. *J. Solid State Chem.* **2017**, *246*, 113–118. [CrossRef]
17. Chen, L.; Shen, L.; Nie, P.; Zhang, X.; Li, H. Facile hydrothermal synthesis of single crystalline $TiOF_2$ nanocubes and their phase transitions to TiO_2 hollow nanocages as anode materials for lithium-ion battery. *Electrochim. Acta* **2012**, *62*, 408–415. [CrossRef]
18. Reddy, M.V.; Madhavi, S.; Rao, G.V.S.; Chowdari, B.V.R. Metal oxyfluorides $TiOF_2$ and NbO_2F as anodes for Li-ion batteries. *J. Power Sources* **2006**, *162*, 1312–1321. [CrossRef]
19. Reddy, M.V.; Rao, G.V.S.; Chowdari, B.V.R. Metal Oxides and Oxysalts as Anode Materials for Li Ion Batteries. *Chem. Rev.* **2013**, *113*, 5364–5457. [CrossRef] [PubMed]
20. Zhou, P.; Yu, J.; Nie, L.; Jaroniec, M. Dual-dehydrogenation-promoted catalytic oxidation of formaldehyde on alkali-treated Pt clusters at room temperature. *J. Mater. Chem. A* **2015**, *3*, 10432–10438. [CrossRef]
21. Nie, L.; Yu, J.; Li, X.; Cheng, B.; Liu, G.; Jaroniec, M. Enhanced Performance of NaOH-Modified Pt/TiO_2 toward Room Temperature Selective Oxidation of Formaldehyde. *Environ. Sci. Technol.* **2013**, *47*, 2777–2783. [CrossRef] [PubMed]

22. Gopalakrishnan, S.; Zampieri, A.; Schwieger, W. Mesoporous ZSM-5 zeolites via alkali treatment for the direct hydroxylation of benzene to phenol with N_2O. *J. Catal.* **2008**, *260*, 193–197. [CrossRef]
23. Wu, Y.; Tian, F.; Liu, J.; Song, D.; Jia, C.; Chen, Y. Enhanced catalytic isomerization of α-pinene over mesoporous zeolite beta of low Si/Al ratio by NaOH treatment. *Microporous Mesoporous Mater.* **2012**, *162*, 168–174. [CrossRef]
24. Wang, Z.; Lv, K.; Wang, G.; Deng, K.; Tang, D. Study on the shape control and photocatalytic activity of high-energy anatasetitania. *Appl. Catal. B Environ.* **2010**, *100*, 378–385. [CrossRef]
25. Niu, L.; Zhang, Q.; Liu, J.; Qian, J.; Zhou, X. TiO_2 nanoparticles embedded in hollow cube with highly exposed {001} facets: Facile synthesis and photovoltaic applications. *J. Alloys Compd.* **2016**, *656*, 863–870. [CrossRef]
26. He, M.; Wang, Z.; Yan, X.; Tian, L.; Liu, G.; Chen, X. Hydrogenation effects on the lithium ion battery performance of $TiOF_2$. *J. Power Sources* **2016**, *306*, 309–316. [CrossRef]
27. Iwata, T.; Watanabe, A.; Iseki, M.; Watanabe, M.; Kandor, H. Strong Donation of the Hydrogen Bond of Tyrosine during Photoactivation of the BLUF Domain. *J. Phys. Chem. Lett.* **2011**, *2*, 1015–1019. [CrossRef]
28. Ning, Y. *Structural Identification of Organic Compounds and Organic Spectroscopy*; Science Press: Beijing, China, 2000; ISBN 978-7-03-0074-126.
29. Zhang, Y.; Zhang, Q.; Xia, T.; Zhu, D.; Chen, Y.; Chen, X. The influence of reaction temperature on the formation and photocatalytic hydrogen generation of (001) faceted TiO_2 nanosheets. *ChemNanoMat* **2015**, *1*, 270–275. [CrossRef]
30. Vaiano, V.; Sannino, D.; Almeida, A.R.; Mul, G.; Ciambelli, P. Investigation of the Deactivation Phenomena Occurring in the Cyclohexane Photocatalytic Oxidative Dehydrogenation on MoOx/TiO_2 through Gas Phase and in situ DRIFTS Analyses. *Catalysts* **2013**, *3*, 978–997. [CrossRef]
31. Samsudin, E.M.; Hamid, S.B.A.; Basirun, W.J.; Centi, G. Synergetic effects in novel hydrogenated F-doped TiO_2 photocatalysts. *Appl. Surf. Sci.* **2016**, *370*, 380–393. [CrossRef]
32. Ding, X.; Hong, Z.; Wang, Y.; Lai, R.; Wei, M. Synthesis of square-like anatase TiO_2 nanocrystals based on $TiOF_2$ quantum dots. *J. Alloys Compd.* **2013**, *550*, 475–478. [CrossRef]
33. Nishikiori, H.; Hayashibe, M.; Fujii, T. Visible Light-Photocatalytic Activity of Sulfate-Doped Titanium Dioxide Prepared by the Sol−Gel Method. *Catalysts* **2013**, *3*, 363–377. [CrossRef]
34. Kowalska, E.; Remita, H.; Colbeau-Justin, C.; Hupka, J.; Belloni, J. Modification of Titanium Dioxide with Platinum Ions and Clusters: Application in Photocatalysis. *J. Phys. Chem. C* **2008**, *112*, 1124–1131. [CrossRef]
35. Park, H.; Choi, W. Photocatalytic Reactivities of Nafion-Coated TiO_2 for the Degradation of Charged Organic Compounds under UV or Visible Light. *J. Phys. Chem. B* **2005**, *109*, 11667–11674. [CrossRef] [PubMed]